



Design, synthesis and SAR of novel glucokinase activators

Zacharia S. Cheruvallath^{a,*}, Stephen L. Gwaltney II^{b,†}, Mark Sabat^a, Mingnam Tang^a, Jun Feng^{c,†}, Haixia Wang^a, Joanne Miura^a, Prasuna Guntupalli^{d,†}, Andy Jennings^a, David Hosfield^{e,†}, Bumsup Lee^{f,†}, Yiqin Wu^{g,†}

^aTakeda California, 10410 Science Center Drive, San Diego, CA 92121, USA

^bGlobal Blood Therapeutics, 400 East Jamie Court, Suite 101, South San Francisco, CA 94080, USA

^cWellspring Biosciences, 3210 Merryfield Row, San Diego, CA 92121, USA

^dRQX Pharmaceuticals, 11099 North Torrey Pines Road, Suite 290, La Jolla, CA 92037, USA

^eBen May Cancer Institute, University of Chicago, USA

^fKolon Life Science, Inc., 7FL Kolon Tower Annex, 38 Byeoryangsangga 2-Ro, Gwacheon-Si, Gyeonggi-Do 427-709, Republic of Korea

^gQuantice Pharmaceuticals Inc., 9393 Towne Centre Drive, Suite 110, San Diego, CA 92121, USA

ARTICLE INFO

Article history:

Received 5 December 2012

Revised 17 January 2013

Accepted 22 January 2013

Available online 4 February 2013

Keywords:

Glucokinase activator

Structure-based drug design

OGTT

Type 2 diabetes

6-Methyl pyridone

ABSTRACT

Guided by co-crystal structures of compounds **15**, **22** and **30**, an SBDD approach led to the discovery of the 6-methyl pyridone series as a novel class of GKAs that potentially activate GK in enzyme and cell assays. Anti-diabetic OGTT efficacy was demonstrated with **54** in a mouse model of type 2 diabetes.

© 2013 Elsevier Ltd. All rights reserved.

Type 2 diabetes (T2D) affects more than 150 million people worldwide and is increasing at an alarming rate due to the ongoing obesity epidemic.¹ While there are several classes of diabetic therapies available, they do not achieve adequate glycemic control, and hence there is a need for the development of safe and effective therapies with a novel mode of action.^{2–5}

Glucokinase (GK), a member of the hexokinase family, is predominantly expressed in the liver, pancreatic β -cells, brain and gut where it catalyzes the phosphorylation of glucose to glucose-6-phosphate.^{6,7} GK plays an important role in the control of whole-body glucose homeostasis by enhancing glucose stimulated insulin release from the pancreatic β -cells and promoting glycogen synthesis in the liver.^{8–10} Glucokinase activators (GKAs) have also been shown to increase hepatic glucose uptake and reduce hyperglycemia in multiple animal models of T2D. GKAs may represent a novel approach for the treatment of T2D.¹¹ Following the initial discovery of an allosteric activator binding site 20 Å removed from the glucose binding site by Grimsby et al.,¹² there have been many publications from pharmaceutical companies targeting this site with GKAs (Fig. 1).^{13–15} There are greater than 100 reports of GKAs

in the patent literature and multiple compounds have been evaluated in the clinic.¹⁶

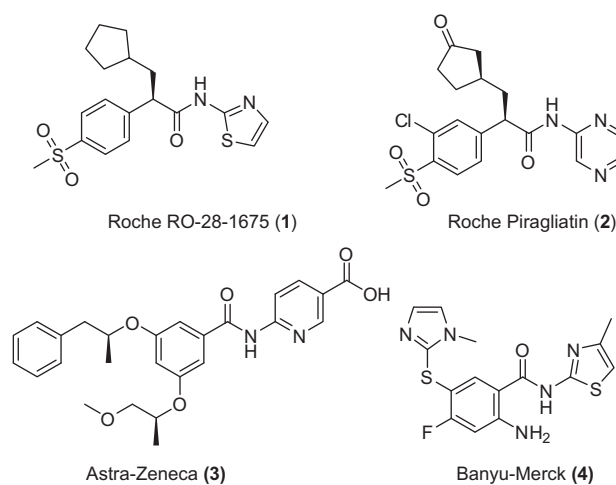


Figure 1. Structures of selected glucokinase activators.

* Corresponding author.

† Present address.

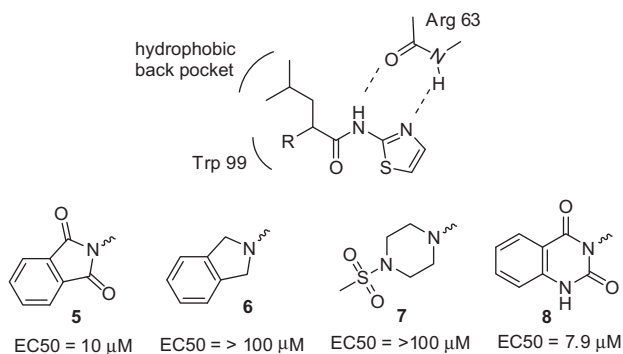


Figure 2. Initially designed GKAs.

All GKAs increase the binding affinity for glucose ($S_{0.5}$);¹⁷ however, they vary in their modulation of the maximum velocity (V_{max}) of glucokinase. We divided our GKAs into three classes based on their effect on GK catalytic activity at saturated glucose concentrations. Activators that enhanced enzyme catalytic turnover at saturated glucose concentrations were denoted Class 1 activators, whereas activators that did not alter enzyme catalytic turnover were called Class 2 and compounds that reduced enzyme catalytic turnover were labeled Class 3. While Class 2 activators may provide benefit to diabetic patients due to activation of GK at moderate glucose concentrations, Class 1 activators may be more effective at high glucose concentrations. Class 3 activators can only activate GK at relatively low glucose concentrations and hence may not be effective in controlling hyperglycemia.

Based on crystal structures of GK both in the absence of glucose and in the presence of glucose and a GKA, Kamata et al. proposed a model to explain the observed positive cooperativity of GK with respect to glucose.¹⁸ In the absence of glucose, or at very low glucose concentrations, GK exists in a low energy, super open, inactive conformation in which the two lobes of the kinase are widely separated and the allosteric binding pocket is not accessible. The open and closed conformations of GK are stabilized by binding of GKA's that result in the increase in affinity of GK for glucose and are favored at high concentrations of glucose. GKAs bind to the allosteric pocket located in the hinge region between the two lobes.

In this Letter, we describe our preliminary efforts to identify and optimize novel, potent and orally bioavailable GKAs for the treatment of T2D.¹⁹ Our analysis of GKAs reported in the literature to bind to the allosteric site of GK,^{11–15} led us to the design of compounds **5–8** as novel GKAs (Fig. 2). Molecular modeling²⁰ of these analogs suggested a complementary fit in the allosteric site of

GK. The energy minimized model indicated hydrogen bonding between the amide NH and the thiazole N with the backbone atoms of Arg63, a hydrophobic interaction of the isopropyl methyl group with the GK back pocket and a π -stacking interactions with Trp99.

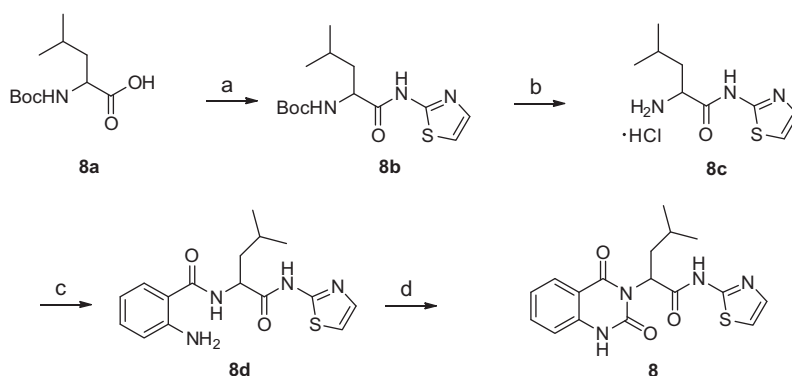
To test our hypothesis, we synthesized compounds **5–8** following either literature precedents¹⁹ or the approach shown in Scheme 1. Coupling of commercially available compound **8a** with 2-aminothiazole gave amide **8b**, which upon treatment with HCl/dioxane gave intermediate **8c**. Amide coupling of **8c** with anthranilic acid gave **8d**, which upon treatment with CDI gave the cyclized target quinazoline-2,4-dione **8**.^{19b} Encouraged by the data for compound **8**, we next aimed to improve the potency of this chemotype by incorporation of substituents on the quinazoline-2,4-dione ring and replacement of the isobutyl chain with groups of increased steric bulk that would interact with the hydrophobic back pocket of GKA.

As seen from the data in Table 1, replacement of the isopropyl group with the cyclohexyl group (compound **9**) improved potency 20-fold, whereas use of the phenyl moiety (compound **10**) led to a >20-fold reduction in potency. With the cyclohexyl group of compound **9** fixed, we examined substituents R^1 and R^2 on the quinazoline-2,4-dione core. Of the analogs examined in this series, compound **16** was the most potent. Analogous to compounds **1**, and **2**, the *S* isomer was the more potent isomer of the pair.^{13,14}

An insight into the binding of these compounds was obtained by an X-ray co-crystal structure of **15** bound in the open form of GK as shown in Figure 3.²⁰ The interactions observed in this co-crystal structure were consistent with our hypothesis. The amide NH and the thiazole N form hydrogen bonds with the backbone atoms of Arg63. The cyclohexylmethyl group forms hydrophobic interactions in the GK back pocket, and the quinazoline-2,4-dione forms aromatic π -stacking interactions with Trp99. Compound **16**, which places the methylsulfonyl group in the same position as that in compound **1**, maintains similar potency consistent with a hydrogen bond interaction of the sulfone oxygen with the side chain of Gln98 as seen in compound **1**.¹²

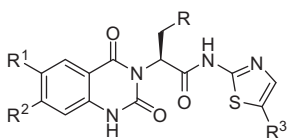
Since attempts to further improve the potency of compound **16** failed, we evaluated alternative heterocyclic scaffolds to replace the quinazoline-2,4-dione core. Molecular modeling²¹ based on our crystal structure of compound **15** suggested that scaffold morphing of the quinazoline-2,4-dione to the quinazoline scaffold could be tolerated. In order to evaluate the potential of this scaffold, we synthesized the quinazolinones by cyclization of the appropriate intermediate (**8d**) by treatment with triethyl orthoformate^{19b} as shown in Scheme 2.

Compound **18** showed potency comparable to that of compound **1** (Table 2). To facilitate further optimization of the scaffold, we obtained a co-crystal structure of compound **22** bound to GK



Scheme 1. Reagents and conditions: (a) isobutyl chloroformate, NMM, 2-aminothiazole, THF; (b) 4 N HCl in dioxane; (c) 2-aminobenzoic acid, HBTU, TEA, DMF; (d) CDI, dioxane, Δ .

Table 1
Selected data for quinazoline-2,4-dione analogs



Compd	R	R ¹	R ²	R ³	EC ₅₀ (μM)	% Maximum activation
1					0.5	98
8^a	<i>i</i> Pr	H	H	H	7.9	67
9	Cyclohexyl	H	H	H	4.0	46
10	Phenyl	H	H	H	>100	0
11	<i>i</i> Pr	H	H	H	50	28
12	Cyclohexyl	H	MeSO ₂	H	1.0	22
13	Cyclohexyl	H	Cl	H	2.0	59
14	Cyclohexyl	OMe	H	H	10	65
15	Cyclohexyl	F	H	H	3.1	127
16^a	Cyclohexyl	H	MeSO ₂	Cl	0.63	37

^a Racemic.

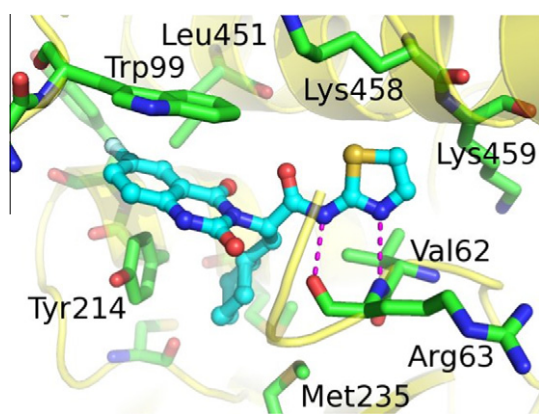


Figure 3. Co-crystal structure of compound **15** in the GK allosteric site.

(Fig. 4).²⁰ In addition to the customary H-bonds to Arg63 and the hydrophobic interaction in the back pocket, when compared to the quinazoline-2,4-dione ring of compound **15**, the F atom of compound **22** is directed towards the backbone NH of Gln98. By binding in this orientation, the C7 atom is directed towards a pocket formed by Val101, Tyr215, and Leu451, suggesting small hydrophobic groups at this position (R²) could increase activator potency.

Consistent with this hypothesis, a 50-fold improvement in potency was obtained by the introduction of a methyl amide at R² of the quinazoline ring and a Cl at R³ of the thiazole ring (**24**). Substitution of the cyclohexyl ring with a THP group led to an 8 to 10-fold reduction in potency (**19** → **20** and **27** → **28**). Although the binding affinity of compound **24** was attractive, it showed low human and rat microsomal stability (*t*_{1/2} < 5 min).

By exploiting in house crystallographic information, molecular modeling²¹ suggested that a ketopiperazine ring would have a

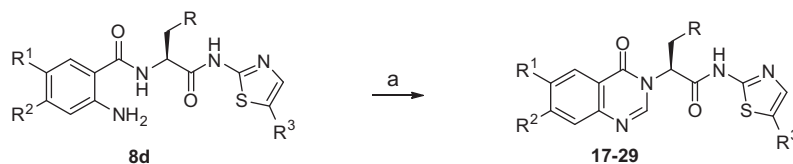
complementary fit in the allosteric site of GK and mimic the quinazoline core to yield potent GKAs.

Analogous to the synthesis of the quinazoline-2,4-diones, the commercially available amino acid **30a** was converted to afford **30c**. Amide coupling of **30c** with a Boc-protected glycine gives intermediate **30d**. After treatment with TFA to remove the Boc group, cyclization to the ketopiperazine intermediate **30e** was achieved by treatment with dibromoethane in the presence of K₂CO₃.^{22–24} The intermediate **30e** was treated with a variety of sulfonyl chlorides to yield compounds **30–42** shown in Scheme 3.

As analysis of the data from Table 3 shows, multiple heterocyclic sulfonamides were well tolerated at position 4 of the ketopiperazine scaffold (compounds **35–40**) with the cyclopentyl sulfonamide being the most potent of the variants made at that position (compound **32**). The 25-fold improvement in potency of compound **32** compared to compound **30** is hypothesized to be due to the hydrophobic interaction of the cyclopentyl group with Pro66 as can be envisioned by the co-crystal structure of compound **30**²⁵ bound in the allosteric site of GK (Fig. 5).²⁰ In addition to the H-bond and hydrophobic interactions, the pucker of the ketopiperazine ring positions the sulfonamide group such that it forms H-bonds with both the OH group of Tyr214 and the backbone amide of Trp99. Interaction with Tyr214 provides an additional interaction in the allosteric site of GK that is not observed with previous compounds. Unfortunately compound **32** also showed low human and rat microsomal stability (*t*_{1/2} < 5 min).

Although the binding affinity of the quinazolinone and ketopiperazine scaffold was attractive, these analogs showed very poor in vitro microsomal stability.

As we continued evaluating alternative templates, the 6-methylpyridone scaffold was docked into the allosteric site of GK. The model suggested a highly complementary fit and so to examine its potential, the 6-methylpyridones were synthesized using the synthetic route shown in Scheme 4. Condensation of commercially



Scheme 2. Reagents and conditions: (a) triethyl orthoformate, TEA, Δ.

Table 2
Selected data for quinazolinone analogs

Compd	R	R ¹	R ²	R ³	EC ₅₀ (μM)	% Maximum activation
1					0.5	98
17	Cyclohexyl	H	H	H	10	72
18	Cyclohexyl	H	MeSO ₂	H	0.5	87
19 ^a	Cyclohexyl	H	CyPrNHCO	Cl	0.12	54
20 ^a	THP	H	CyPrNHCO	Cl	1.2	36
21 ^a	Cyclohexyl	Cl	H	H	2	56
22	Cyclohexyl	F	H	H	4	108
23	Cyclohexyl	Me	H	H	2.5	86
24	Cyclohexyl	H	MeNHCO	Cl	0.079	58
25	Cyclohexyl	H	CyPentylSO ₂	F	0.31	72
26	Cyclohexyl	H	CyPentylISO ₂	Cl	0.4	65
27	Cyclohexyl	H	EtSO ₂	F	0.63	87
28	THP	H	EtSO ₂	F	5	44
29	Cyclopentyl	H	CyPrSO ₂	H	2	44

^a Racemic, Cy = cyclo.

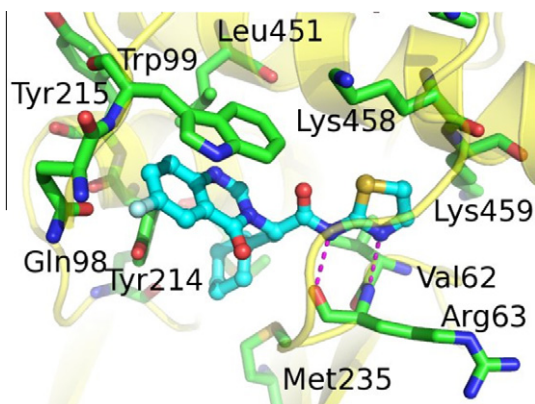
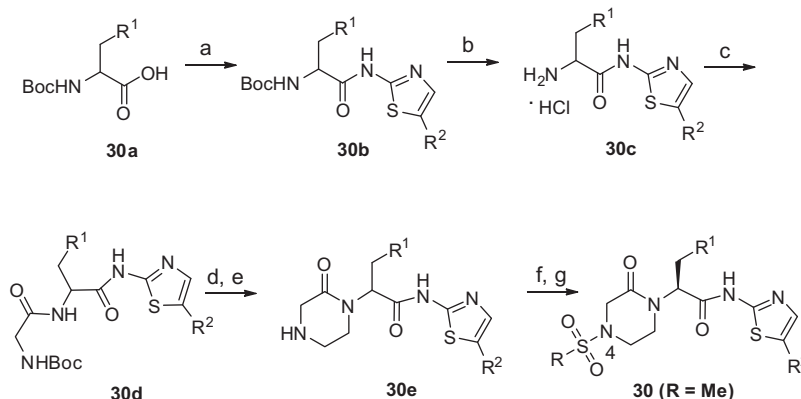


Figure 4. Co-crystal structure of compound **22** in the GK allosteric site.

available 4-hydroxy-6-methyl-2*H*-pyran-2-one with an appropriately substituted amino acid in the presence of a base gave the intermediate **43b**.²⁶ Esterification, followed by treatment with POCl₃ and dimethylaniline in the presence of tetraethyl ammonium chloride gave the 4-chloro-6-methylpyridone intermediate **43c**.²⁷ Displacement of the halide with thiolate followed by oxidation with *m*CPBA gave the sulfone **43d**. Hydrolysis of the ester followed by amide coupling with the substituted 2-aminothiazoles gave the desired 6-methylpyridone analogs.



Scheme 3. Reagents and conditions: (a) thiazol-2-amine, HBTU, TEA, DMF; (b) 4 N HCl in dioxane; (c) 2-((*tert*-butoxycarbonyl)amino)acetic acid, HBTU, TEA, DMF; (d) 4 N HCl in dioxane; (e) 1,2-dibromoethane, K₂CO₃, dioxane, 100 °C; (f) sulfonyl chloride, TEA, DMAP, DCM; (g) chiral HPLC purification.

The 6-methyl pyridone analogs showed binding affinities comparable to the quinazolinone and ketopiperazine analogs (Table 4). In addition, in the enzyme assay, the V_{max} of the 6-methyl pyridone series resembled compound **1** which is a Class 1 activator unlike the ketopiperazines which were found to be Class 2/3 activators. The 6-methylpyridones strike a good balance between potency and V_{max} of glucokinase.

As shown in Table 4, an increase in steric bulk on the sulfone at position 4 of the pyridone led to an 80-fold increase in potency (**43** → **44** → **45**). Unfortunately compound **45** showed low human and rat microsomal stability ($t_{1/2}$ < 5 min). With the cyclopentyl group of compound **45** fixed, we explored a variety of substituents at R and R₂ (**46**–**52**) to improve the microsomal stability of the compounds while maintaining potency without any success. However, while compound **54** was less potent than other compounds in this series, it was found to combine the best balance of GK activation and in vitro DMPK properties and hence was chosen for further profiling in efficacy models. Compound **54** showed a half-life of 120 min, 35 min and 60 min respectively when incubated with MLM, RLM and HLM. Its rat pharmacokinetic profile was characterized by an oral half-life of 5.9 h, clearance of 69 mL/min/kg, volume of distribution of 2.4 L/kg and an oral bioavailability of 36%.

Oral administration of 30 mg/kg of **54** in C57BL/6J mice resulted in a significant glucose lowering effect. In addition, compound **54** administered at an oral dose of 30 mg/kg reduced glucose excursion in an oral glucose tolerance test (OGTT) experiment in ob/ob mice in a manner comparable to that of compound **1** (Fig. 6).

In summary, using co-crystal structures of compounds **15**, **22** and **30**, an SBDD approach led to the discovery of the 6-methylpyridone

Table 3
Selected data for ketopiperazine analogs

Compd	R	R ¹	R ²	EC ₅₀ (μM)	% Maximum activation
1				0.5	98
30^a	Me	Cyhexyl	H	1.6	64
31^a	Cyclopropyl	Cyhexyl	H	0.25	64
32	Cyclopentyl	Cyhexyl	H	0.063	33
33	Cyclopropyl	THP	Cl	0.79	22
34	Me	THP	Cl	2	21
35	3-Cl phenyl	Cyhexyl	H	0.31	36
36	3,5-diF phenyl	Cyhexyl	H	0.2	44
37	3-Me phenyl	Cyhexyl	H	0.2	33
38	2-F,4-Me phenyl	Cyhexyl	H	0.25	39
39	2-Furyl	Cyhexyl	H	0.16	62
40	N-Me pyrazole	Cyhexyl	H	0.31	54
41	Bn	Cyhexyl	H	0.4	25
42	iPr	Cyhexyl	H	1	45

^a Racemic, cyhexyl = cyclohexyl.

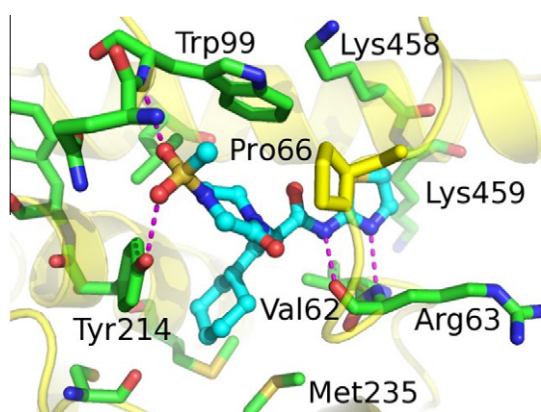
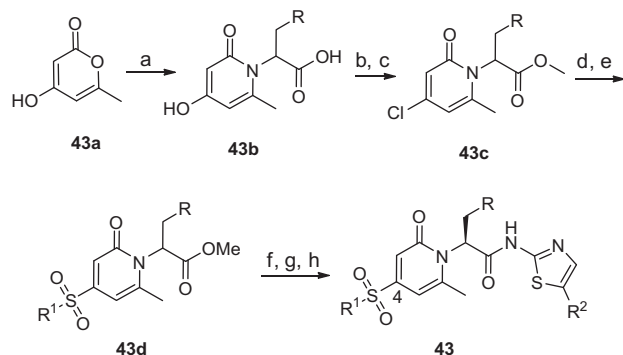


Figure 5. Co-crystal structure of compound **30** in the GK allosteric site.



Scheme 4. Reagents and conditions: (a) amino acid, 1 N NaOH, reflux; (b) MeOH, H₂SO₄, reflux; (c) POCl₃, Et₃NCl, dimethylaniline, ACN, 80 °C; (d) thiol, NaH, DMSO, 80 °C; (e) mCPBA, DCM; (f) 1 M LiOH, dioxane; (g) aminothiazole, HBTU, TEA, DMF; (h) chiral HPLC purification.

series as a novel class of GKAs. Example **54** from the 6-methylpyridone series was assessed in an in vivo model of T2D and demonstrated potent activity. Future reports will describe further modification of the 6-methylpyridones for optimization of in vivo properties.

Acknowledgements

The authors appreciate the drug discovery expertise of Jeffrey Stafford. We thank Robert Skene, Gyorgy Snell, Lisa Rahbaek, Pamela Farrell and Beverly Knight for their valuable experimental

Table 4
Selected data for 6-methyl pyridone analogs

Compd	R	R ¹	R ²	EC ₅₀ (μM)	% Maximum activation
1				0.5	98
43	Cyclohexyl	Me	H	6.3	125
44	Cyclohexyl	Et	H	2	117
45	Cyclohexyl	Cypentyl	H	0.079	88
46^a	iPr	Cypentyl	H	0.79	73
47^a	Cyclopropyl	Cypentyl	H	1.6	40
48^a	Cyclopentyl	Cypentyl	H	0.2	75
49^a	THP	Cypentyl	F	1	64
50^a	n-pr	Cypentyl	H	1.6	55
51	THP	Cypentyl	Cl	0.16	52
52	THP	Cypentyl	F	0.5	68
53	Cyclopentyl	Cypropyl	F	0.63	109
54	THP	Cypropyl	Cl	1.2	77
55	Cyclopentyl	Cypropyl	Cl	0.16	90

^a Racemic, cypentyl = cyclopentyl, cypropyl = cyclopropyl.

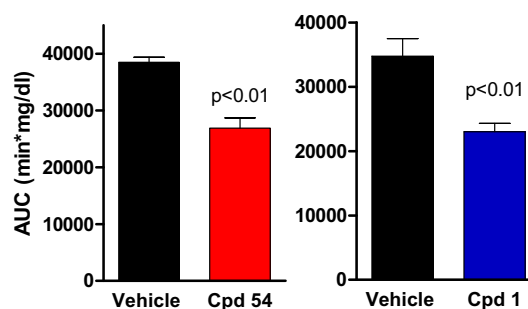


Figure 6. Glucose AUCs of **1** and **54** following an oral administration to C57BL/6J mice (dose 30 mg/kg for both compounds).

assistance. The X-ray crystallography data reported here is based on research conducted at the Advanced Light Source (ALS). ALS is supported by the Director, Office of Science, Office of Basic Energy Sciences, Materials Sciences Division, of the U.S. Department of Energy (DOE) under Contract No. DE-AC03-76SF00098 at Lawrence Berkeley National Laboratory. We thank the staff at ALS for their excellent support in the use of the synchrotron beam lines. The authors would like to thank Matt Marx and Gavin Hirst for help with reviewing the document.

References and notes

- Tadayyon, M.; Smith, S. A. *Expert Opin. Invest. Drugs* **2003**, *12*, 307.
- Turner, R. C.; Cull, C. A.; Frighi, V.; Holmann, R. *J. Am. Med. Assoc.* **2005**, *1999*, 281.

3. Nathan, D. M. N. *Eng. J. Med.* **2002**, *347*, 1342.
4. Gershell, L. *Nat. Rev. Drug Disc.* **2005**, *4*, 367.
5. Bell, D. S. *Treat. Endocrinol.* **2004**, *3*, 67.
6. Matschinsky, F. M. *Diabetes* **2002**, *51*, S394.
7. *Frontiers in Diabetes*; Matschinsky, F. M., Magnuson, M. A., Eds.; Karger: Basel, 2004; p 1. Vol. 16.
8. Gloyn, A. I.; Odili, S.; Zelent, D.; Buettger, C.; Castleden, H. A.; Steele, A. M.; Stride, A.; Shiota, C.; Magnusson, M. A.; Lorini, R.; d'Annunzio, G.; Stanley, C. A.; Kwagh, J.; van Schaftingen, E.; Veigha da Cunha, M.; Barbetti, F.; Dunten, P.; Han, Y.; Grimsby, J.; Taub, R.; Ellard, S.; Hattersley, A. T.; Matschinsky, F. M. *J. Biol. Chem.* **2005**, *280*, 14105.
9. Leighton, B.; Atkinson, A.; Coghlan, M. P. *Biochem. Soc. Trans.* **2005**, *33*, 371.
10. Zelent, D.; Najafi, H.; Odili, S.; Buettger, C.; Weik-Collins, H.; Li, C.; Doliba, N.; Grimsby, J.; Matschinsky, F. M. *Biochem. Soc. Trans.* **2005**, *33*, 306.
11. Sarabu, R.; Grimsby, J. *Curr. Opin. Drug Disc. Dev.* **2005**, *8*, 631.
12. Grimsby, J.; Sarabu, R.; Corbett, W. L.; Haynes, N. E.; Bizzarro, F. T.; Coffey, J. W.; Guertin, K. R.; Hilliard, D. W.; Kester, R. F.; Mahaney, P. E.; Marcus, L.; Qi, L.; Spence, C. L.; Teng, J.; Magnuson, M. A.; Chu, C. A.; Dvorozniak, M. T.; Matschinsky, F. M.; Grippo, J. F. *Science* **2003**, *301*, 370.
13. Fyfe, M. C. T.; Procter, M. P. *Drugs Future* **2009**, *34*, 641.
14. Matschinsky, F. M. *Nat. Rev. Drug Disc.* **2009**, *8*, 399.
15. Coghlan, M.; Leighton, B. *Expert Opin. Invest. Drugs* **2008**, *17*, 145.
16. Sarabu, R.; Berthel, S. J.; Kester, R. F.; Tilley, J. W. *Expert Opin. Ther. Patents* **2008**, *18*, 759.
17. $S_{0.5}$ is the concentration of glucose at which the GK activity reaches half of its maximum activity.
18. Kamata, K.; Mitsuya, M.; Nishimura, T.; Eiki, J.; Nagata, Y. *Structure* **2004**, *12*, 429.
19. Patent applications describing our GKAs have been published. Full experimental procedures for all analogs in this Letter are contained within the patent applications: (a) Cao, S. X.; Feng, J.; Gwaltney, S. L.; Hosfield, D. J.; Skene, R. J.; Stafford, J. A.; Tang, M. US200072811942.; (b) Cheruvallath, Z.; Feng, J.; Guntupalli, P.; Gwaltney, S. L.; Kaldor, S. W.; Miura, J.; Sabat, M.; Tang, M. US2007213349.; (c) Cheruvallath, Z.; Feng, J.; Guntupalli, P.; Gwaltney, S. L.; Miura, J.; Sabat, M.; Tang, M.; Wang, H. WO2008079787, WO2008/16107A2.
20. PDB ID code for compound **15** is 41SF, compound **22** is 41SE and compound **30** is 41SG.
21. Molecular Operating Environment (MOE), Chemical Computing Group Inc., Montreal, Canada H3A 2R7, <http://www.chemcomp.com>.
22. Reyes, A.; Regla, I.; Fragoso, M. C.; Vallejo, L. A.; Demare, P.; Jimenez-Vazquez, H. A.; Ramirez, Y.; Juaristi, E.; Tamariz, J. *Tetrahedron* **1999**, *55*, 11187.
23. Mohamed, N.; Bhatt, U.; Just, G. *Tetrahedron Lett.* **1998**, 8213.
24. Khan, N. M.; Cano, M.; Balasubramanian, S. *Tetrahedron Lett.* **2002**, 2439.
25. Crystallographic studies with the racemic compound **30** produced a co-complex structure with only the *S* isomer of the compound.
26. Castillo, S.; Ouadahi, H.; Herault, V. *Bull. Soc. Chim. Fr.* **1982**, *2*, 257.
27. Bressi, J. C.; Chloe, J.; Hough, M. T.; Buchner, F. S.; Van Voorhis, W.; Verlinde, C.; Hol, W.; Gelb, M. H. *J. Med. Chem.* **2000**, *43*, 4135.